European Journal of Chemistry

View Journal Online
View Article Online

Synthesis, crystal structure, characterization, Hirshfeld surface, and DFT studies of a dimeric copper complex of 3-methylpyridine-2-carboxylic acid

Anupam Datta [1], Vikas Kumar Dakua [1], Debadrita Roy [2], Purak Das [3], Satadal Paul [4], Kanak Roy [1], Subhra Mishra [5], and Mahendra Nath Roy [2,*]

[1] *Department of Chemistry, Alipurduar University, Alipurduar, 736122, India*
[2] *Department of Chemistry, University of North Bengal, Siliguri, 734013, India*
[3] *Department of Chemistry, Rishi Bankim Chandra College, North 24 Parganas, 743165, India*
[4] *Department of Chemistry, Bangabasi Morning College, Kolkata, 700009, India*
[5] *Department of Chemistry, Kharagpur College, Kharagpur, 721305, India*

* *Corresponding author at: Department of Chemistry, University of North Bengal, Siliguri, 734013, India.*
e-mail: mahendraroy2002@yahoo.co.in (M.N. Roy).

RESEARCH ARTICLE

10.5155/eurjchem.17.1.62-68.2725

Received: 14 November 2025
Received in revised form: 20 December 2025
Accepted: 5 February 2026
Published online: 31 March 2026
Printed: 31 March 2026

KEYWORDS

DFT
MOF
SCXRD
Cu(II) complex
Hirshfeld topology
Hydrothermal synthesis

ABSTRACT

A Cu(II) complex with 3-methylpyridine-2-carboxylic acid, formulated as $(C_{14}H_{12}CuN_2O_4)_n$ (Complex I), was synthesized and characterized using infrared spectroscopy (IR), thermogravimetric analysis (TGA) and single-crystal X-ray diffraction. The crystal structure of Complex I is monoclinic, space group $P2_1/c$, with unit-cell parameters a = 4.9892(6) Å, b = 15.002(2) Å, c = 8.5649(12) Å, and volume V = 638.49(15) Å^3. The Cu(II) center adopts a quasioctahedral coordination geometry and is located at a crystallographic inversion center. Density functional theory (DFT) calculations and Hirshfeld surface analysis revealed that noncovalent interactions, including H···O, H···C, and π···π contacts, play a significant role in stabilizing the three-dimensional supramolecular architecture of the complex.

Cite this: *Eur. J. Chem.* **2026**, *17(1)*, 62-68 **Journal website**: www.eurjchem.com

1. Introduction

Coordination polymers with transition metals have been increasingly explored over the past two decades, particularly for their promising properties and applications in areas such as catalysis and porous materials [1-5]. Due to their small size, the first row transition-metal ions can easily coordinate with the N and O atoms, typically forming simple structures. These metal-organic frameworks have important applications in biological processes, catalysis, magnetochemistry, photochemistry, and analytical chemistry [6-9]. The coordination chemistry of copper(II) complexes is diverse and shows promising biological activities.

Picolinic acid, with its versatile structure, is an important ligand in this context. The development of metal-based compounds using this type of ligand gained momentum in the 1980s. Its versatility in coordination with transition metals has shown promise for anticancer applications [10-12]. The biocatalytic properties of copper complexes, especially those with organic acids, have sparked interest. Picolinate complexes are notable for their ambiguous structures and multiple bonding possibilities. Carboxylate compounds are notable for their potential as coordination ligands for transition metals, exhibiting multiple coordination modes due to the bonding capabilities of the carboxylate group and the varying oxidation states of the metals [13]. Nitrogen-based ligands are widely used in coordination chemistry for the development of complexes, to understand the relationships between structure, spectroscopy, and catalysis in metalloenzymes [14]. Picolinic acid is a versatile ligand that has attracted attention for its flexibility in coordination. Its complexes with various metal ions are used in nutritional supplements and pharmaceuticals, showing potential in the treatment of conditions such as arteriosclerosis and liver disorders [15,16].

Our study reports the synthesis and comprehensive characterization of a new dimeric Cu(II) complex of 3-methylpicolinic acid. The structural features of the complex were investigated using single-crystal X-ray diffraction and infrared (IR) spectroscopy, and further analyzed through density functional theory (DFT) calculations.

https://dx.doi.org/10.5155/eurjchem.17.1.62-68.2725

Table 1. Crystal data collection and structure refinement for Complex I.

CCDC reference number	2239934
Empirical formula	$C_{14}H_{12}CuN_2O_4$
Moiety formula	$C_{14}H_{12}CuN_2O_4$
Formula weight	335.80
Crystal system	Monoclinic
Space group	$P2_1/c$
Colour	Blue
Size, mm	0.20 × 0.20 × 0.15
Unit cell dimensions	
	a = 4.9892(6)Å
	b = 15.002(2)Å
	c = 8.5649(12)Å
	β = 95.145(6)°
Volume Å^3	638.49(15)
Z	2
Density (calculated), mg/m^3	1.747
Absorption coefficient, mm^{-1}	1.728
F(000)	342
Data collection	
Temperature, K	296(2)
Theta range for data collection	3.617° to 28.329°
Index ranges	$-6 \le h \le 3$
	$-19 \le k \le 19$
	$-11 \le l \le 11$
Reflections collected	7546
Unique reflections	1543
Observed reflections (>2$\sigma(I)$)	1240
R_{int}	0.0298
Completeness to θ, %	25.242°, 99.7
Absorption correction	Multi-scan / (SADABS; Bruker 2000)
	T_{min} = 0.715, T_{max} = 0.772
Refinement	
Refinement method	Full-matrix least-squares on F^2
Data/restraints/parameters	1543 / 0 / 98
Goodness-of-fit on F^2	0.934
Final R indices [I > 2σ(I)]	R_1 = 0.0290, wR_2 = 0.0797
R indices (all data)	R_1 = 0.0405, wR_2 = 0.0898
Largest diff. peak and hole	0.457 and -0.269 e.Å^{-3}

In addition, the bonding characteristics, frontier molecular orbitals (HOMO-LUMO), and molecular surface properties were explored using Hirshfeld surface analysis and DFT methods, providing insights into the electronic structure and intermolecular interactions of the complex.

2. Experimental

2.1. Materials and instrumentation

Analytical grade chemicals were used for the synthesis, including 3-methylpyridine-2-carboxylic acid (99%) and $Cu(NO_3)_2{\cdot}3H_2O$ (99%), both purchased from Sigma-Aldrich and used without further purification. Infrared (IR) spectra were recorded on a Nicolet 6700 FT-IR spectrophotometer over the range 4000-400 cm^{-1}. Single-crystal X-ray diffraction data were collected on a Bruker AXS Kappa Apex-II CCD diffractometer equipped with graphite-monochromated Mo Kα radiation (λ = 0.71073 Å). The thermal stability of the complex was evaluated using thermogravimetric analysis (TGA) under a nitrogen atmosphere (20 mL/min) with a heating rate of 2 °C/min, from room temperature to 1300 °C, on a PerkinElmer Diamond TGA/DTA STA 6000 instrument.

2.2. Synthesis of complex I

3-Methylpicolinic acid (0.1371 g) and $Cu(NO_3)_2{\cdot}3H_2O$ (0.2416 g) were thoroughly ground together using an agate mortar. The resulting mixture was transferred to a 10 mL Teflon-lined autoclave, followed by the addition of 5 mL deionized water, and stirred for approximately 30 minutes to ensure a homogeneous suspension. The autoclave was then sealed and heated at 140 °C for 72 hours. After the reaction, the system was gradually cooled to room temperature for 12 hours. The pH of the suspension remained stable at around 6 throughout the process. Block-shaped, pale-colored crystals formed, which were collected by filtration, washed with water and ethanol, and dried under ambient conditions for several hours. The obtained product corresponded to a 70% yield based on the metal precursor.

2.3. Single-crystal X-ray diffraction (SCXRD) measurements

Single-crystal X-ray diffraction data was collected on a Bruker Smart Apex II diffractometer using Mo Kα radiation (λ = 0.71073 Å) and a graphite monochromator. Data reduction and unit cell refinement were performed using the SAINT program. The crystal structure was solved and refined using SHELXL-97. All non-hydrogen atoms were refined anisotropically, while hydrogen atoms were positioned geometrically and refined using a Fourier difference map. Molecular graphics and structural representations were generated using Mercury, SHELXL-97, and ORTEP-3 [17-19].

2.4. Computational methodology

Density functional theory (DFT) calculations were performed to investigate the electronic structure of the Cu(II) complex. Geometry optimizations were carried out using the metahybrid TPSSh functional [20] in combination with relativistic basis sets implemented via the zeroth order regular approximation (ZORA), retaining one-center terms. ZORA-recontracted def2-TZVP basis sets were applied to all atoms except C and H, for which ZORA-def2-SVP basis sets were used [21-24]. To minimize errors associated with the resolution of identity (RI) and chain of spheres (COSX) approximations for Coulomb and exact exchange integrals, a large decontracted SARC/J auxiliary basis set was used [25-27]. Noncovalent interactions were considered using atom-pairwise dispersion corrections with Becke-Johnson damping (D3BJ) [28].

Table 2. Bond lengths for complex I *.

Atom	Atom	Length (Å)	Atom	Atom	Length (Å)
C1	C2	1.390(3)	C5	N1	1.332(3)
C1	C7	1.520(3)	C7	O1	1.285(2)
C1	N1[1]	1.349(2)	C7	O2	1.217(2)
C2	C3	1.397(3)	N1	C1[1]	1.349(2)
C2	C6	1.504(3)	N1	Cu1	1.9591(16)
C3	C4[1]	1.374(3)	O1	Cu1	1.9357(14)
C4	C3[1]	1.374(3)	Cu1	N1[1]	1.9591(16)
C4	C5	1.377(3)	Cu1	O1[1]	1.9357(14)

* Symmetry code: [1] 1-*x*, 1-*y*, 2-*z*.

Table 3. Bond angles for complex I *.

Atom	Atom	Atom	Angle (°)	Atom	Atom	Atom	Angle (°)
C2	C1	C7	125.72(18)	O2	C7	O1	125.1(2)
N1[1]	C1	C2	121.85(19)	C1[1]	N1	Cu1	113.23(13)
N1[1]	C1	C7	112.36(16)	C5	N1	C1[1]	120.38(17)
C1	C2	C3	116.31(19)	C5	N1	Cu1	126.32(13)
C1	C2	C6	124.1(2)	C7	O1	Cu1	115.21(13)
C3	C2	C6	119.61(19)	N1[1]	Cu1	N1	180.0
C4[1]	C3	C2	121.5(2)	O1[1]	Cu1	N1	83.18(6)
C3[1]	C4	C5	118.3(2)	O1	Cu1	N1[1]	83.18(6)
N1	C5	C4	121.44(19)	O1	Cu1	N1	96.81(6)
O1	C7	C1	114.69(17)	O1[1]	Cu1	N1[1]	96.82(6)
O2	C7	C1	120.16(19)	O1	Cu1	O1[1]	180.0

* Symmetry code: [1] 1-*x*, 1-*y*, 2-*z*.

Table 4. Torsion angles for complex I *.

A	B	C	D	Angle (°)	A	B	C	D	Angle (°)
C1	C2	C3	C4[1]	-2.1(3)	C7	C1	C2	C3	-172.08(19)
C1	C7	O1	Cu1	-10.0(2)	C7	C1	C2	C6	9.9(3)
C2	C1	C7	O1	-169.66(19)	N1[1]	C1	C2	C3	4.9(3)
C2	C1	C7	O2	13.1(3)	N1[1]	C1	C2	C6	-173.19(19)
C3[1]	C4	C5	N1	-2.4(4)	N1[1]	C1	C7	O1	13.1(3)
C4	C5	N1	C1[1]	-0.3(3)	N1[1]	C1	C7	O2	-164.13(19)
C4	C5	N1	Cu1	176.35(17)	O2	C7	O1	Cu1	167.11(18)
C6	C2	C3	C4[1]	176.0(2)					

* Symmetry code: [1] 1-*x*, 1-*y*, 2-*z*.

Table 5. C–H···*Cg* interactions in complex I *.

Bond	H···*Cg* (Å)	H-Perp (Å)	Gamma (°)	X - H··· *Cg* (°)
C6–H(6C)···*Cg*3[i]	2.66	-2.63	8.36	165

* Symmetry codes: (i) -1+*x*, *y*, *z*. Cg3 is the centroid of the N1–C5 ring.

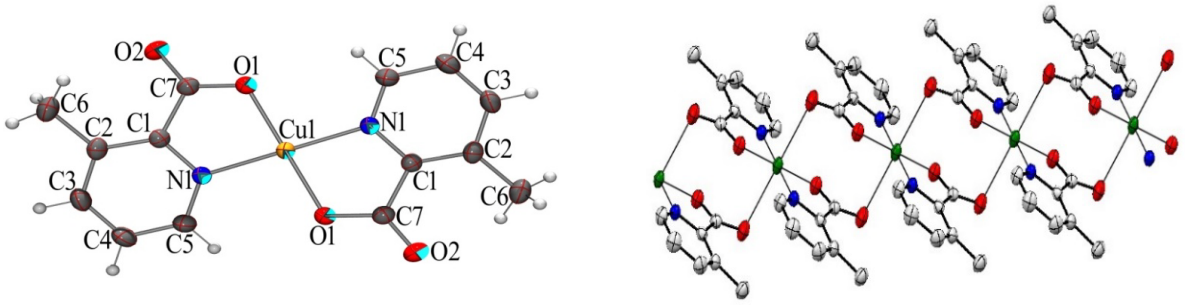

(a) (b)

Figure 1. ORTEP diagrams of Complex I: (a) and (b) show the molecular structure with atom labels and polymeric architecture. Thermal ellipsoids are drawn with a 50% probability.

All calculations were carried out in ORCA (version 5.3.0) [29]. The Hirshfeld surface analysis was performed using Crystal Explorer 17.5 to evaluate the nature of intermolecular interactions and crystal packing [30].

3. Results and discussion

3.1. Structure of complex I

SC-XRD analysis revealed that complex I (Figure 1) adopts a polymeric structure with a molecular formula $(C_{14}H_{12}CuN_2O_4)_n$. The complex crystallizes in the monoclinic $P2_1/c$ space group with $Z = 2$. The crystallographic data (crystal parameters, data collection, and refinements) of Complex I are given in Table 1. Selected bond lengths, bond angles, and torsion angles are listed in Tables 2-4. The molecule experiences three nonclassical hydrogen bonding interactions as presented in Table 5 and shown in Figure 2.

The metal ion in complex I adopts a quasi-octahedral coordination environment, situated at a crystallographic inversion center. In the equatorial plane, there are two bidentate ligands in *trans* orientation, which chelate the metal ion through pyridine N and carboxylate O atoms, generating five-membered rings. The quasi-octahedral geometry is completed by two *O* atoms from different picolinate ligands occupying the axial positions with a bond length (Cu1-O2 = 2.715(14) Å).

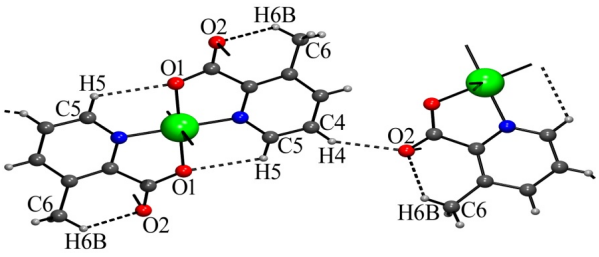

Figure 2. Intermolecular and intramolecular hydrogen bonding in complex I.

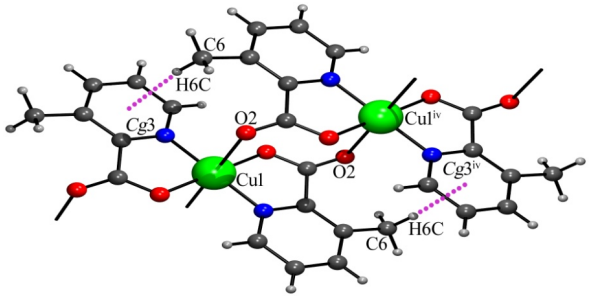

Figure 3. C–H···*Cg* interactions in complex I. *Symmetry codes: (iv) -1+x, y, z.*

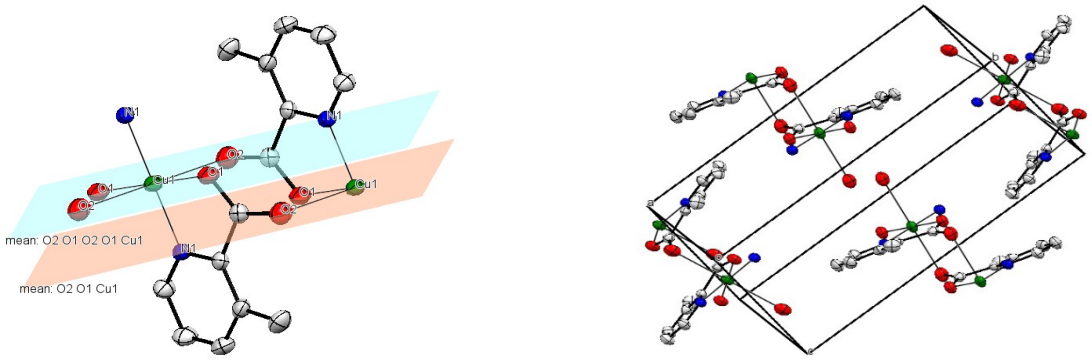

(a) (b)

Figure 4. Quasi-octahedral coordination geometry (a) and crystal packing diagram (b) of Complex I. Color scheme: Cu – green, O – red, N – blue, C – grey.

Although the length of the bond exceeds the normal Cu-O bond length, this molecule experiences such bonding interactions due to the strong C–H···*Cg* interactions (Figure 3, Table 5), which actually polymerize the molecular assembly.

The longer axial bond length (Cu1-O2 = 2.715(14) Å) than the lengths of the equatorial bond (Cu1-O1 = 1.9357(14) Å and Cu1-N1 = 1.9591 (16) Å) reflects the commonly observed Jahn-Teller effect in octahedral copper complexes. The bond angles presented in Table 3 reveal that the title compound exhibits a distorted octahedral geometry, similar to that found in analogous metal complexes [31,32]. Hydrogen bonds between the picolinate apical O atoms and neighbouring molecules, along with strong C–H···*Cg* interactions, link the molecules into a 3D framework (Figure 4).

3.2. Infrared studies

Upon complexation, the disappearance of the 2607-2152 cm^{-1} bands, attributed to O-H-N hydrogen bonding in 3-picolinic acid, confirms that the nitrogen and carboxylate oxygen atoms are involved in coordination [33]. The Cu(II) complex exhibits $\nu_{as}(COO^-)$ and $\nu_s(COO^-)$ bands at 1629 and 1339 cm^{-1}, with the Δν separation providing information about the carboxylate coordination mode [34]. A Δν value of 290 cm^{-1} suggests unidentical carboxylate coordination in the Cu(II) complex [35]. The shift of the ν(C=N) band from 1595 to 1578 cm^{-1} further supports complexation. Coordination of the ligand to the metal center through the pyridine nitrogen and carboxylate oxygen is also evidenced by the presence of characteristic ν(C-H) near 2970 cm^{-1} broad stretching bands.

3.3. Thermal gravimetric analysis

The TGA curve of complex I shows a sharp decline from 300 to 350 °C which may be attributed to the loss of two molecules of 3-methyl picolinic anion and the final product being the CuO residue, formed between 400-800 °C.

3.4. DFT study and Hirshfeld surface analysis

The Cu(II) complex is optimized in square pyramidal geometry with the unpaired electron at the $d_{x^2-y^2}$ orbital (Figure 5). The energy of SOMO and LUMO has been calculated and found to be −4.472 and −2.196 eV, respectively, and the $\Delta E = (E_{LUMO}\text{-}E_{SOMO})$ for the same is found to be 2.276 eV, indicating that complex I is stable [36]. The negative value of μ of the above complex I indicates its thermal resistivity, air stability, and does not continuously decompose into its elemental form. The CIF was input into Crystal Explorer 17.5 to generate Hirshfeld surfaces and 2D fingerprint plots [37].

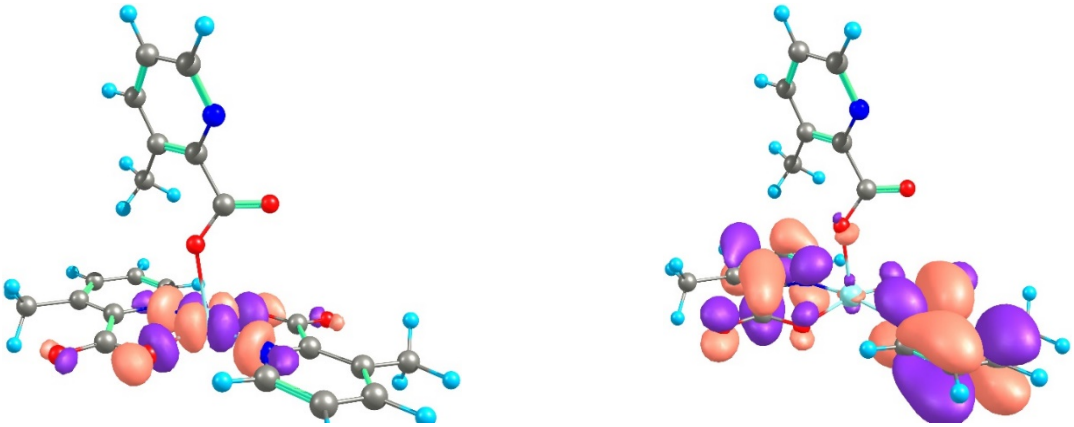

(a) (b)

Figure 5. Schematic of SOMO (a) and LUMO (b), obtained as the quasi-restricted orbital in the optimized geometry, Color code: Green-Cu, Cyan-H, Blue-N, Red-O, Grey-C.

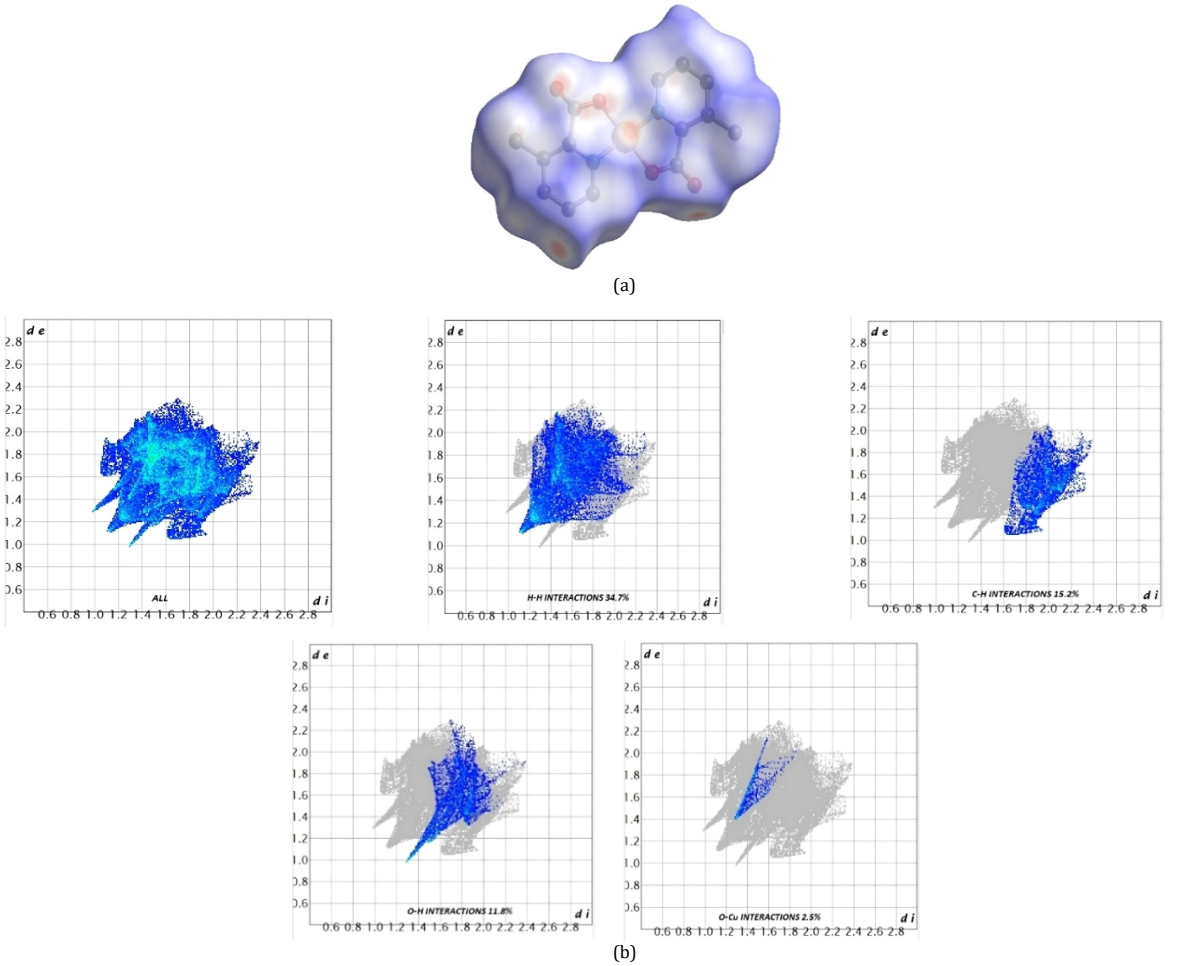

(a) (b)

Figure 6. (a) Normalized distance (d_{norm}) plot showing intermolecular interactions; red regions indicate close contacts and the blue regions indicate longer contacts. (b) Two-dimensional fingerprint (2D-FP) plot highlighting the proportion of interactions inside and outside the van der Waals surface.

A color scale from -0.7080 Å (red) to 1.5685 Å (blue) was applied to the d_{norm} surface of Complex I, and transparency was used to enhance visibility of the molecular details. The d_{norm} values were derived from the combination of the d_e and d_i distances. It is given by Equation 1,

$$d_{norm} = \frac{\left(d_i - r_i^{vdW}\right)}{r_i^{vdW}} + \frac{\left(d_e - r_e^{vdW}\right)}{r_e^{vdW}} \quad (1)$$

Here, d_e represents the distance from a surface point to the closest nucleus outside, while d_i represents the distance to the closest nucleus inside. r_i^{vdw} and r_e^{vdw} denote the van der Waals radii of the internal and external atoms. Hirshfeld surface analysis provides a visual representation of intermolecular interactions, complementing single-crystal X-ray diffraction results [38].

The Hirshfeld surfaces are mapped with d_{norm} in Figure 6, highlighting close contacts as red spots, with increasing brightness for shorter distances. These interactions are quantified in 2D fingerprint plots (Figure 6). These close contacts are quantified and visualized in 2D fingerprint plots, with d_i and d_e distances ranging from 1.0 to 2.8 (Figure 6). H···H, C···H, and O···H contacts dominate the Hirshfeld surface, appearing as symmetrical narrow wings, and comprise 34.7, 15.2, and 11.8% of the total surface area for complex I. While O···Cu and N···Cu interactions are minimal, the molecular packing is largely influenced by other significant interactions, along with some minor but contributing interactions.

4. Conclusions

The present study demonstrates that complex I exhibits a quasi-octahedral coordination geometry around the copper(II) center. The metal ion is stabilized by two bidentate methyl picolinic acid ligands in the equatorial plane, forming five-membered chelate rings, while two axial oxygen atoms from separate ligands complete the octahedral environment. The elongation of the axial Cu–O bonds relative to the equatorial bonds reflects the typical Jahn–Teller distortion observed in the octahedral copper complexes.

Strong intermolecular interactions, including C–H···π and hydrogen bonding, promote polymerization of molecular units into a three-dimensional supramolecular network, enhancing structural stability. Computational studies and thermogravimetric analysis further confirm that complex I possesses significant thermal stability. These findings underscore the ability of methyl picolinic acid ligands to stabilize higher oxidation states of copper, which may be advantageous for applications in catalysis and materials chemistry.

Acknowledgements

We gratefully acknowledge the support from the University of North Bengal, Department of Chemistry, for computational studies; SAIF, Cochin University of Science and Technology, for single-crystal X-ray diffraction (SC-XRD) measurements; and the Central Instrumentation Facility (CIF), Lovely Professional University, for IR and thermogravimetric (TGA) analyses.

Supporting information

CCDC-2239934 contains the supplementary crystallographic data for this paper. These data can be obtained free of charge via www.ccdc.cam.ac.uk/data_request/cif, or by e-mailing data_request@ccdc.cam.ac.uk, or by contacting The Cambridge Crystallographic Data Centre, 12 Union Road, Cambridge CB2 1EZ, UK; fax: +44(0)1223-336033.

Disclosure statement

Conflict of interest: The authors declare that they have no conflict of interest.
Ethical approval: All ethical guidelines have been adhered to.
Sample availability: Samples of the compound are available from the author.

CRediT authorship contribution statement

Conceptualization: Anupam Datta, Vikas Kumar Dakua; Methodology: Anupam Datta, Vikas Kumar Dakua; Software: Satadal Paul, Purak Das; Validation: Satadal Paul, Subhra Mishra; Formal Analysis: Anupam Datta, Vikas Kumar Dakua; Investigation: Anupam Datta, Debadrita Roy; Resources: Anupam Datta, Vikas Kumar Dakua; Data Curation: Vikas Kumar Dakua, Kanak Roy; Writing - Original Draft: Vikas kumar Dakua, Kanak Roy; Writing - Review and Editing: Vikas Kumar Dakua, Kanak Roy; isualization: Debadrita Roy, Purak Das; Funding acquisition: Mahendra Nath Roy; Supervision: Mahenbra Nath Roy, Vikas Kumar Dakua; Project Administration: Mahenbra Nath Roy, Vikas Kumar Dakua.

ORCID and Email

Anupam Datta
anupamdatta27@gmail.com
https://orcid.org/0000-0003-4888-1954
Vikas Kumar Dakua
dakuavikas7@gmail.com
https://orcid.org/0000-0002-3843-7166
Debadrita Roy
debadrita2015@gmail.com
https://orcid.org/0009-0004-7848-6538
Purak Das
purakdas@gmail.com
https://orcid.org/0000-0001-6229-8306
Satadal Paul
satadal2008@gmail.com
https://orcid.org/0000-0001-6425-0285
Kanak Roy
kanakroynbu@gmail.com
https://orcid.org/0000-0002-2075-3056
Subhra Mishra
subhra_apd@yahoo.com
https://orcid.org/0009-0007-9426-5403
Mahendra Nath Roy
mahendraroy2002@yahoo.co.in
https://orcid.org/0000-0002-7380-5526

References

[1]. Matsuda, R.; Kitaura, R.; Kitagawa, S.; Kubota, Y.; Belosludov, R. V.; Kobayashi, T. C.; Sakamoto, H.; Chiba, T.; Takata, M.; Kawazoe, Y.; Mita, Y. Highly controlled acetylene accommodation in a metal–organic microporous material. *Nature* **2005**, *436* (7048), 238–241.
[2]. Chui, S. S.; Lo, S. M.; Charmant, J. P.; Orpen, A. G.; Williams, I. D. A Chemically Functionalizable Nanoporous Material [Cu3(TMA)2(H2O)3]n. *Science* **1999**, *283* (5405), 1148–1150.
[3]. Moulton, B.; Zaworotko, M. J. From Molecules to Crystal Engineering: Supramolecular Isomerism and Polymorphism in Network Solids. *Chem. Rev.* **2001**, *101* (6), 1629–1658.
[4]. Blake, A. J.; Champness, N. R.; Hubberstey, P.; Li, W.; Withersby, M. A.; Schröder, M. Inorganic crystal engineering using self-assembly of tailored building-blocks. *Coord. Chem. Rev.* **1999**, *183* (1), 117–138.
[5]. Horcajada, P.; Serre, C.; Maurin, G.; Ramsahye, N. A.; Balas, F.; Vallet-Regí, M.; Sebban, M.; Taulelle, F.; Férey, G. Flexible Porous Metal-Organic Frameworks for a Controlled Drug Delivery. *J. Am. Chem. Soc.* **2008**, *130* (21), 6774–6780.
[6]. O'Brien, P. Reactivity of co-ordination compounds in the solid state. Part 1. Mixed-ligand complexes of oxalate and 2,2′-bipyridyl with copper(II), their preparation, interconversion, and novel solid-state reactivity. *J. Chem. Soc. Dalton Trans.* **1981**, 1540–1543.
[7]. Bencini, A.; Di Vaira, M.; Fabretti, A. C.; Gatteschi, D.; Zanchini, C. Anisotropic exchange in transition-metal dinuclear complexes. 2. Crystal and molecular structure and EPR spectra of a dinuclear copper oxamidato complex. *Inorg. Chem.* **1984**, *23* (11), 1620–1623.
[8]. Gregson, A.; Doddrell, D.; Pegg, D. Electron spin relaxation in solutions of transition metal ions with S ≥ 1. Conditions where the Redfield limit is valid. *Aust. J. Chem.* **1978**, *31* (3), 469–473.
[9]. Schmitz, W. International Tables for X-ray Crystallography, vol. IV (Ergänzungsband). Herausgegeben von der International Union of Crystallography. The Kynoch Press, Birmingham, England, 1974, 366 Seiten einschließlich Tabellen und Sachwortverzeichnis. *Cryst. Res. Technol* **1975**, *10* (11), 336 https://doi.org/10.1002/crat.19750101116.
[10]. Chohan, Z. H.; Shad, H. A. Structural elucidation and biological significance of 2-hydroxy-1-naphthaldehyde derived sulfonamides and their first row d-transition metal chelates. *J. Enzyme Inhib. Med. Chem.* **2008**, *23* (3), 369–379.
[11]. Chohan, Z. H.; Shad, H. A.; Nasim, F. Synthesis, characterization and biological properties of sulfonamide-derived compounds and their transition metal complexes. *Applied Organomet. Chem.* **2009**, *23* (8), 319–328.
[12]. Celestine, M. J.; Bullock, J. L.; Boodram, S.; Rambaran, V. H.; Holder, A. A. Interesting properties of p-, d-, and f-block elements when coordinated with dipicolinic acid and its derivatives as ligands: their use as inorganic pharmaceuticals. *Rev. Inorg. Chem.* **2015**, *35* (2), 57–67.
[13]. Tamer, O.; Sarıboğa, B.; Uçar, O.; Büyükgüngör, O. Spectroscopic characterization, X-ray structure, antimicrobial activity and DFT calculations of novel dipicolinate copper(II) complex with 2,6-pyridinedimethanol. *Spectrochim. Acta A: Mol. Biomol. Spectrosc.* **2011**, *84* (1), 168–177.

[14]. Adams, H.; Bailey, N. A.; Crane, J. D.; Fenton, D. E.; Latour, J.; Williams, J. M. Manganese(II) and iron(III) complexes of the tridentate ligands bis(benzimidazol-2-ylmethyl)-amine (L^1) and -methylamine (L^2). Crystal structures of $[MnL^1(CH_3CO_2)_2]$, $[FeL^2Cl_3]$, and $[Fe_2L^1_2(\mu\text{-}O)\{\mu\text{-}(CH_3)_3CCO_2\}_2][ClO_4]_2$. *J. Chem. Soc. Dalton Trans.* **1990**, 1727–1735.
[15]. Nakajima; Suzuki, K. K. Jpn. Kokai Tokkyo Koho JP 91-23767, 5, 1992.
[16]. Abe, H. Jpn. Kokai Tokkyo Koho JP 91-142904, 7, 1992.
[17]. Sheldrick, G. M. A short history of *SHELX*. *Acta Crystallogr A. Found Crystallogr* **2007**, *64* (1), 112–122.
[18]. Farrugia, L. J. *ORTEP*-3 for Windows - a version of*ORTEP*-III with a Graphical User Interface (GUI). *J. Appl. Crystallogr.* **1997**, *30* (5), 565–565.
[19]. Bruno, I. J.; Cole, J. C.; Edgington, P. R.; Kessler, M.; Macrae, C. F.; McCabe, P.; Pearson, J.; Taylor, R. New software for searching the Cambridge Structural Database and visualizing crystal structures. *Acta Crystallogr. B. Struct. Sci.* **2002**, *58* (3), 389–397.
[20]. Staroverov, V. N.; Scuseria, G. E.; Tao, J.; Perdew, J. P. Comparative assessment of a new nonempirical density functional: Molecules and hydrogen-bonded complexes. *J. Chem. Phys.* **2003**, *119* (23), 12129–12137.
[21]. van Lenthe, E.; Snijders, J. G.; Baerends, E. J. The zero-order regular approximation for relativistic effects: The effect of spin–orbit coupling in closed shell molecules. *J. Chem. Phys.* **1996**, *105* (15), 6505–6516.
[22]. van Lenthe, E.; Baerends, E. J.; Snijders, J. G. Relativistic total energy using regular approximations. *J. Chem. Phys.* **1994**, *101* (11), 9783–9792.
[23]. Pantazis, D. A.; Chen, X.; Landis, C. R.; Neese, F. All-Electron Scalar Relativistic Basis Sets for Third-Row Transition Metal Atoms. *J. Chem. Theory Comput.* **2008**, *4* (6), 908–919.
[24]. Schäfer, A.; Huber, C.; Ahlrichs, R. Fully optimized contracted Gaussian basis sets of triple zeta valence quality for atoms Li to Kr. *J. Chem. Phys.* **1994**, *100* (8), 5829–5835.
[25]. Neese, F.; Wennmohs, F.; Hansen, A.; Becker, U. Efficient, approximate and parallel Hartree–Fock and hybrid DFT calculations. A 'chain-of-spheres' algorithm for the Hartree–Fock exchange. *Chem. Phys.* **2009**, *356* (1-3), 98–109.
[26]. Weigend, F. Accurate Coulomb-fitting basis sets for H to Rn. *Phys. Chem. Chem. Phys.* **2006**, *8* (9), 1057.
[27]. Sproviero, E. M.; Gascón, J. A.; McEvoy, J. P.; Brudvig, G. W.; Batista, V. S. Quantum Mechanics/Molecular Mechanics Study of the Catalytic Cycle of Water Splitting in Photosystem II. *J. Am. Chem. Soc.* **2008**, *130* (11), 3428–3442.
[28]. Grimme, S.; Ehrlich, S.; Goerigk, L. Effect of the damping function in dispersion corrected density functional theory. *J. Comput. Chem.* **2011**, *32* (7), 1456–1465.
[29]. Neese, F. Software update: the ORCA program system, version 4.0. *WIREs Comput Mol Sci* **2017**, *8* (1), 1327 https://doi.org/10.1002/wcms.1327.
[30]. Spackman, M. A.; Jayatilaka, D. Hirshfeld surface analysis. *CrystEngComm* **2009**, *11* (1), 19–32.
[31]. Okabe, N.; Muranishi, Y.; Odoko, M. Cobalt(II), nickel(II) and copper(II) complexes of isoquinoline-3-carboxylate. *Acta Crystallogr. C* **2004**, *60*, m345–m347.
[32]. Okabe, N.; Muranishi, Y.; Wada, Y. 5-*n*-Butylpyridine-2-carboxylate–copper(II) and –iron(III) complexes. *Acta Crystallogr. C. Cryst. Struct. Commun.* **2002**, *58* (10), m511–m513.
[33]. Kukovec, B.; Kakša, M.; Popović, Z. Synthesis and Characterization of a Copper(II) Complex with 6-Hydroxypicolinic Acid and 3-Picoline. *Croat. Chem. Acta* **2012**, *85* (4), 479–483.
[34]. Żurowska, B.; Ochocki, J.; Mroziński, J.; Ciunik, Z.; Reedijk, J. Synthesis, spectroscopic and magnetostructural evidence for the formation of Cu(II) complexes of pyridyl-2-carboxylate (2-pca) and quinolyl-2-carboxylate (2-qca) as a result of a novel oxidative P-dealkylation reaction of diethyl 2-pyridylmethylphosphonate (2-pmpe) and diethyl 2-quinolylmethylphosphonate (2-qmpe) ligands. *Inorg. Chim. Acta* **2004**, *357* (3), 755–763.
[35]. Jacimovic, Z.; Kosovic, M.; Novakovic, S.; Giester, G.; Radovic, A. Synthesis and crystal structure of Cu(II) and Co(II) complexes with 1,3-dimethyl-pyrazole-5-carboxylic acid ligand. *J. Serb. Chem. Soc.* **2015**, *80* (7), 867–875.
[36]. Fukui, K. Theory of Orientation and Stereoselection. *React. Struct. Concepts Org. Chem.* **1975**, https://doi.org/10.1007/978–3–642–61917–5.
[37]. McKinnon, J. J.; Jayatilaka, D.; Spackman, M. A. Towards quantitative analysis of intermolecular interactions with Hirshfeld surfaces. *Chem. Commun.* **2007**, 3814–3816.
[38]. Hirshfeld, F. L. Bonded-atom fragments for describing molecular charge densities. *Theoret. Chim. Acta* **1977**, *44* (2), 129–138.